2D Phased Array Driving Scheme Optimization for Ultrasound Neuromodulation

Aqamolaei, Masoumeh; Costa, Tiago L.

DOI
10.1109/UFFC-JS60046.2024.10793494

Publication date
2024

Document Version
Final published version

Published in
IEEE Ultrasonics, Ferroelectrics, and Frequency Control Joint Symposium, UFFC-JS 2024 - Proceedings

2D Phased Array Driving Scheme Optimization for Ultrasound Neuromodulation

1st Masoumeh Aqamolaei
Microelectronics Department
Delft University of Technology
Delft, the Netherlands
M.Aqamolaei@tudelft.nl

2nd Tiago L. Costa
Microelectronics Department
Delft University of Technology
Delft, the Netherlands
T.M.L.daCosta@tudelft.nl

2024 IEEE Ultrasonics, Ferroelectrics, and Frequency Control Joint Symposium (UFFC-JS) | 979-8-3503-7190-1/24/$31.00 ©2024 IEEE | DOI: 10.1109/UFFC-JS60046.2024.10793494

***Abstract*—Developing an implantable/wearable 2D ultrasound phased array for ultrasound neuromodulation poses several challenges, including power requirements for driving the piezoelectric transducers to generate sufficient pressure at the focal spot. Therefore, minimizing power consumption is crucial to minimize excessive thermal dissipation and to ensure long-term usability without frequent charging or battery replacement. Prior work has improved efficiency based on transducer fabrication and circuit design optimizations. To further address this issue, we propose a new approach to minimize power consumption by tailoring the driving amplitude of each element in a 2D phased array based on their individual contribution to the focal spot pressure.**

***Index Terms*—Phased array, Ultrasound, Neuromodulation, Optimization**

I. Introduction

In recent years, neuromodulation-based therapies have emerged to address several neurological diseases [1], such as Parkinson's disease and depression. While these therapies have the common goal of activating or inhibiting neuronal activity towards the desired therapeutic outcome, they can drastically differ in terms of many other properties, such as spatial resolution and coverage, depth of penetration, form factor, and non-invasiveness. Fig. 1 illustrates a comparison of different neuromodulation modalities concerning these properties, where it can be seen that, among all, ultrasound-based neuromodulation modalities show great promise. Transcranial focused ultrasound (tFUS) has been demonstrated to attain significant penetration depths by utilizing ultrasound frequencies below the MHz range, albeit at the cost of reduced spatial resolution, requiring bulky transducers and electronics. Conversely, microscopic ultrasound stimulation (μUS) positioned beneath the skull can leverage ultrasound frequencies within the MHz range, thereby affording enhanced spatial resolution capabilities while maintaining its small form factor. However, to fully explore the benefits of μUS towards deep brain stimulation at high spatial coverage and resolution, we would need a power-efficient system to ensure long-term usability as a wearable or implantable system without frequent charging or battery replacement and without leading to excessive thermal dissipation. Prior work has improved efficiency based on transducer fabrication [2] [3] [4] [5] and circuit design optimizations [6] [7] [8] [9] [10]. To further address this issue, we propose a new approach to minimize power consumption by optimizing the driving scheme of each transducer. In ultrasound neuromodulation, each element in the transducer array is typically driven with the same voltage, and focusing is achieved by means of beamforming. However, due to the directivity of each element, their individual contribution to the focal spot pressure differs along the array. In this work, we propose a new driving scheme for therapeutic ultrasound 2D arrays, where the driving voltage of each transducer is defined based on their individual contribution to the focal spot pressure to minimize power consumption. This approach was optimized employing simulations with the k-Wave Matlab toolbox [11]. This work is organized as follows: Section II discusses the methodology used to lower power consumption. Section III presents the simulation results. Section IV concludes the paper.

This work was supported by the project UPSIDE (ID 101070931), which has received funding within the framework of Horizon EIC 2021 Pathfinder Challenges by the European Union.

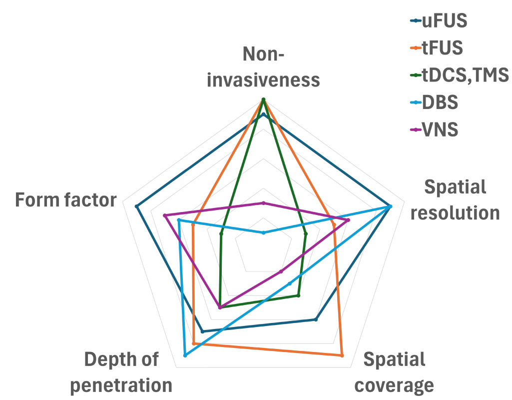

Fig. 1: Comparison of different neuromodulation approaches in terms of spatial resolution, spatial coverage, depth of penetration, form factor, and non-invasiveness.

II. Methods

A. Underlying Concept

In a 2D phased array of transducers, the contribution of each element in the focal spot pressure depends on the directivity

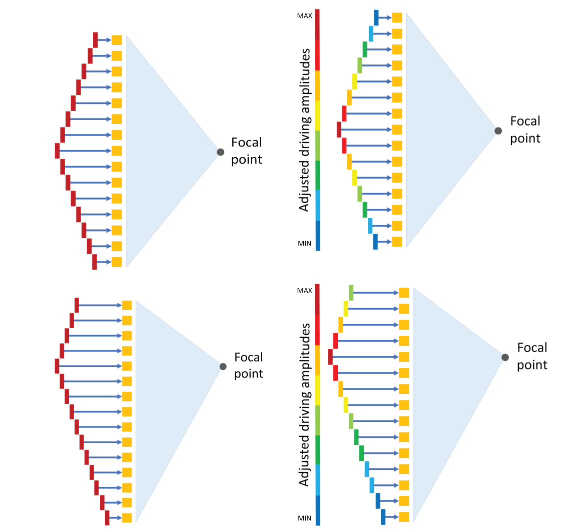

(a) (b)

Fig. 2: Conceptual implementation of the proposed method (a) all the elements in a phased array are driven with the same amplitude regardless of the location of the focal point. (b) driving amplitude of elements is adjusted based on the location of the focal point.

function of each transducer. The directivity in a phased array is a function of element width(w), pitch(p), acoustic angle, and distance. Hence, with equal size and pitch of elements in a phased array, the contribution of each element to the final pressure at the focal point varies based on the location of the element in the array, focal depth, and the steering angle. By knowing the contribution of each element in the phased array, higher driving amplitudes can be assigned to the elements with higher contribution and lower driving amplitude to the elements with lower contribution, hence avoiding the excess power consumption from the latter. Fig. 2 shows the simplified concept of this hypothesis of adapting driving amplitude based on the location of the focal point in a 1D phased array; the same methodology can be applied to a 2D phased array.

The k-Wave toolbox of MATLAB has been used for 3D time-domain simulation of 2D phased arrays. In the proposed study, different apertures, focal depths, and steering angles were investigated for a case study of a conceptual array tailored for *in vivo* experiments in rodents. For that reason, the maximum aperture is limited by 6 mm due to space limitations (craniotomy) and, with a frequency of 5MHz, which offers a good compromise between absorption and spatial resolution, this results in a 2D array with 40 x 40 elements. In the following sections, the contribution of each element in a phased array is first discussed, followed by an exploration of the element contributions to optimize the driving scheme to minimize power consumption. Further, a discussion of how the power consumption of the array is estimated for different conditions is presented.

B. Contribution of Elements

To obtain a map of the contribution of elements in a phased array, first, the phase delay of each element in a phased array should be calculated based on the focal depth and steering angle. Then, the pressure at the focal spot is computed by turning on each element at a time and applying a sinusoidal signal with the same amplitude and phase delay as if in a phased array. Since, at each iteration, just one element is turned on, the computed pressure at the focal spot is considered as the contribution of that element in the focal spot. By repeating this process for each individual element, a complete map of the pressure contribution of elements to the focal spot can be obtained for different focal depths and steering angles. Fig. 3 depicts the contribution map for a phased array with a 6mm aperture (40 by 40 elements with a pitch of 150μm for a 5MHz transducer array) for three different focal depths (3mm, 6mm, and 12mm) with and without steering. The results show that, at greater focal depths, all elements contribute more evenly to the focal spot due to similar distances from the focal point. However, when the beam is steered, contributions vary more as elements on one side are more impacted by directivity and attenuation losses.

C. Optimization of the Driving Scheme

In a phased array, all elements are typically driven by a signal with the same amplitude (V_m), with phase delays applied to each element to focus the beam at a specific depth. These phase delays are calculated based on the distance from each element to the focal point [12]. However, using the same amplitude for all elements can result in power inefficiency. Firstly, element directivity dictates that elements with larger steering angles contribute less to the focal spot. Secondly, elements positioned farther from the focal point generate ultrasound waves that experience greater attenuation as they propagate more through the medium to reach the focal depth, reducing their contribution to the pressure at the focal spot. By knowing the normalized contribution of each element (CE) in the array for the desired focal depth and steering angle, the driving scheme can be optimized such that the elements with less contribution are driven with a lower voltage. To estimate the effect of this process on the focal pressure, the k-Wave toolbox of MATLAB was used to simulate a map of the contribution of each element to the focal spot pressure. With the obtained contribution map, each element in the i^{th} row and j^{th} column was assigned driving amplitudes of $V_(i,j) = CE_(i.j) \times V_m$ where V_m corresponds to the maximum driving voltage in actual implementation and $CE_(i.j)$, as mentioned earlier, is the normalized contribution of the element in the i^{th} row and j^{th} column to the pressure at the focal point.

D. Power Consumption Estimation

To calculate the power consumption, the electrical model of the ultrasound transducers should be defined. Fig. 4 shows the simplified model of an ultrasound transducer using the Butterworth Van Dyke(BVD) model. In the resonance frequency of

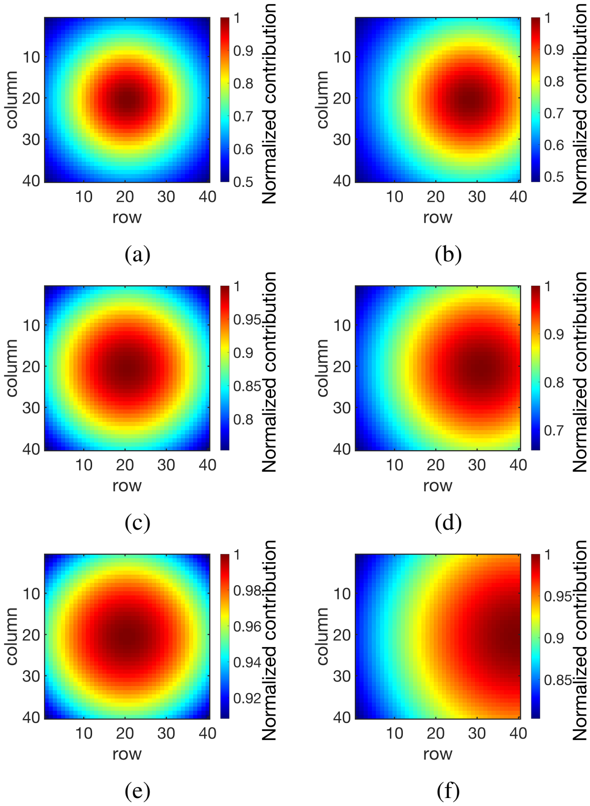

Fig. 3: Simulation results showing the normalized contribution of each element in a 40x40 2D phased array with a 6mm aperture and for different focal depths and steering angles. The normalized contribution of each element is represented in the color of each pixel according to the shown color bars: (a) 3mm focal depth and no steering. (b) 3mm focal depth and 15-degree steering. (c) 6mm focal depth and no steering. (d) 6mm focal depth and 15-degree steering. (e) 12mm focal depth and no steering. (f) 12mm focal depth and 15-degree steering.

the transducer ($f_r = \frac{1}{2\pi\sqrt{L_s C_s}}$), the model can be simplified to $R_S \| C_0$. By considering PZT transducers in this study, C_0 is often small enough to assume that $R_S << \frac{1}{jWC_0}$, meaning that R_S is the dominant element in the model consuming power. The power consumption by R_S corresponds to the power converted from the electrical to the acoustic domain [13]; hence, to simplify, each element is modeled as a resistor. Hereby, the power consumption of one element equals:

$$P_{i,j} = \frac{V_{(i,j)}^2}{R_S} \tag{1}$$

and the total power consumption of the array equals:

$$P_T = \sum_{i=1}^{N} \sum_{j=1}^{M} \frac{V_{(i,j)}^2}{R_S} \tag{2}$$

where N is the number of rows and M is the number of columns in the phased array.

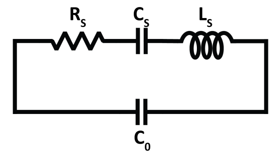

Fig. 4: Butterworth Van Dyke(BVD) model of the transducer

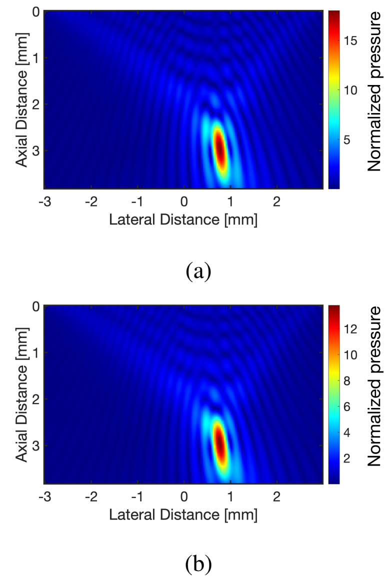

Fig. 5: Comparison of the beam profile (a). elements are driven with the same amplitude (b). elements are driven by adjusted amplitude based on their contribution to the focal point pressure.

III. Results and Discussion

Fig. 5 presents the simulated beam profile of an ultrasound phased array both with and without applying the proposed optimization method. By adjusting the driving amplitudes of the array elements based on their individual contributions to the focal spot, the beam profile remains unchanged. However, as illustrated in Fig. 5, while the pressure at the focal spot decreases, this reduction primarily results from lowering the driving amplitude of the elements that contribute less significantly to the focal spot.

Fig. 6 shows the results of the proposed optimization method for various apertures and F-numbers[1], with simulations performed at steering angles of zero and 15 degrees. The results demonstrate that the reduction in power consumption is consistently higher than the corresponding decrease in focal spot pressure. Additionally, the results show that as the focal depth increases, the difference between the power consumption reduction and the focal spot pressure decrease narrows. This behavior is expected, as indicated in Fig. 3, where at greater focal depths, the relative contribution of each element to the

[1]In ultrasound applications, the F-number is defined as the ratio of focal depth to aperture width.

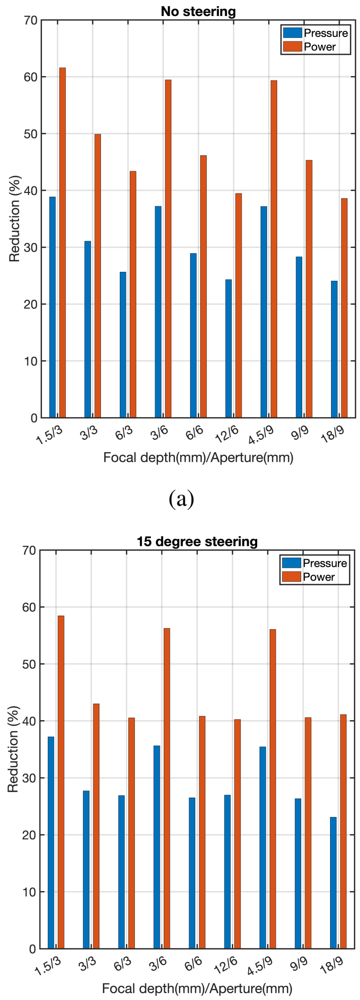

(a)

(b)

Fig. 6: Comparison of the power consumption reduction and focal spot pressure drop after optimizing element driving amplitudes in a phased array (a) no steering. (b) 15-degree steering.

focal spot becomes more uniform due to their similar distances from the focal point. However, when the beam is steered, the disparity between the contributions of individual elements increases as elements on one side are more affected by their directivity and attenuation losses. Finally, Fig. 6 highlights that, for a fixed F-number across different apertures, the power consumption and focal spot pressure reduction remain nearly identical. This suggests that the method is robust across a range of aperture sizes, maintaining efficiency and consistent pressure reduction irrespective of aperture variations. This study shows that having the ability to individually control the driving voltage amplitude of each transducer in a phased array can lead to higher power efficiency; however, this comes with the cost of more complex driving electronics, for which the power efficiency should also be considered in future implementations.

IV. Conclusion

In this paper, we introduced a novel approach to optimize the driving scheme of elements in a phased array by employing a contribution map that quantifies each element's impact on the final pressure at the focal spot. By adjusting the driving amplitudes based on element location, focal depth, and steering angle, we effectively minimized the system's power consumption. The simulation results demonstrate that this optimization strategy allows for a decrease in power consumption that exceeds the reduction in focal pressure at the focal spot compared to the typical driving scheme. This enhancement in power efficiency is particularly advantageous for neuromodulation devices, where it enables more efficient operation by tailoring the driving voltage for each channel based on the focal spot location. Overall, our approach offers a promising pathway to achieve lower power consumption while maintaining effective focal performance.

References

[1] B. Davidson, A. Bhattacharya, C. Sarica, G. Darmani, N. Raies, R. Chen, and A. M. Lozano," Neuromodulation techniques - From non-invasive brain stimulation to deep brain stimulation," Neurotherapeutics, vol. 21, no. 3, 2024.

[2] G. K. Wardhana, M. Mastrangeli and T. L. Costa, "Maximization of Transmitted Acoustic Intensity from Silicon Integrated Piezoelectric Ultrasound Transducers," IEEE International Ultrasonics Symposium (IUS), Venice, Italy, pp. 1-4, 2022.

[3] G. K. Wardhana, T. L. Costa, and M. Mastrangeli, "An Acoustically Transparent Electrical Cap for Piezoelectric Ultrasound Transducers on Silicon," Proceedings, vol. 97 n. 1, 2024.

[4] T. Costa, C. Shi, K. Tien, J. Elloian, F. A. Cardoso and K. L. Shepard, "An Integrated 2D Ultrasound Phased Array Transmitter in CMOS With Pixel Pitch-Matched Beamforming," IEEE Transactions on Biomedical Circuits and Systems, vol. 15, no. 4, pp. 731-742, Aug. 2021

[5] J. S. Letchumanan, S. Gandhi, H. Yin, A. Ramkumar and K. L. Shepard, "A Mechanically Flexible 32-by-32-Element Pitch-Matched Ultrasound Front-End Transceiver with Two-Stage Beamforming for 3D Imaging," 2024 IEEE Custom Integrated Circuits Conference (CICC), Denver, CO, USA, pp. 1-2, 2024.

[6] H. Rivandi and T. L. Costa, "A 2D Ultrasound Phased-Array Transmitter ASIC for High-Frequency US Stimulation and Powering," IEEE Transactions on Biomedical Circuits and Systems, vol. 17, no. 4, pp. 701-712, Aug. 2023.

[7] Y. Xiao, H. Rivandi and T. L. Costa, "An Energy-Efficient High-Voltage Pulser for High-Frequency Ultrasound Medical Applications," IEEE Biomedical Circuits and Systems Conference (BioCAS), Toronto, ON, Canada, pp. 1-5, 2023.

[8] I. Bellouki, N. Rozsa, Z. -Y. Chang, Z. Chen, M. Tan and M. Pertijs, "6.4 A Resonant High-Voltage Pulser for Battery-Powered Ultrasound Devices," 2024 IEEE International Solid-State Circuits Conference (ISSCC), San Francisco, CA, USA, pp. 106-108, 2024.

[9] M. Gourdouparis et al., "An Ultrasound-Powering TX with a Global Charge-Redistribution Adiabatic Drive Achieving 69% Power Reduction and 53° Maximum Beam Steering Angle for Implantable Applications," 2024 IEEE International Solid-State Circuits Conference (ISSCC), San Francisco, CA, USA, pp. 102-104, 2024.

[10] C. Seok, O. J. Adelegan, A. Ö. Biliroğlu, F. Y. Yamaner and Ö. Oralkan, "A Wearable Ultrasonic Neurostimulator—Part II: A 2D CMUT Phased Array System With a Flip-Chip Bonded ASIC," IEEE Transactions on Biomedical Circuits and Systems, vol. 15, no. 4, pp. 705-718, 2021.

[11] Bradley Treeby (2024). k-Wave (https://github.com/ucl-bug/kwave/releases/tag/v1.4.0), GitHub. Retrieved September 13, 2024.

[12] S. J. Ilham, Z. Kashani and M. Kiani, "Design and Optimization of Ultrasound Phased Arrays for Large-Scale Ultrasound Neuromodulation," IEEE Transactions on Biomedical Circuits and Systems, vol. 15, no. 6, pp. 1454-1466, Dec. 2021.

[13] A. A. Vives, "Piezoelectric transducers and applications," Springer Berlin Heidelberg, 2008.